LANGMUIR

pubs.acs.org/Langmuir Article

Unraveling How Ethanol-Induced Conformational Changes Affect BSA Protein Adsorption onto Silica Surfaces

Jia Ying Brenda Tan,[§] Bo Kyeong Yoon,[§] Gamaliel Junren Ma, Tun Naw Sut, Nam-Joon Cho,* and Joshua A. Jackman*

Cite This: *Langmuir* 2020, 36, 9215−9224 Read Online

ACCESS | Metrics & More | Article Recommendations | Supporting Information

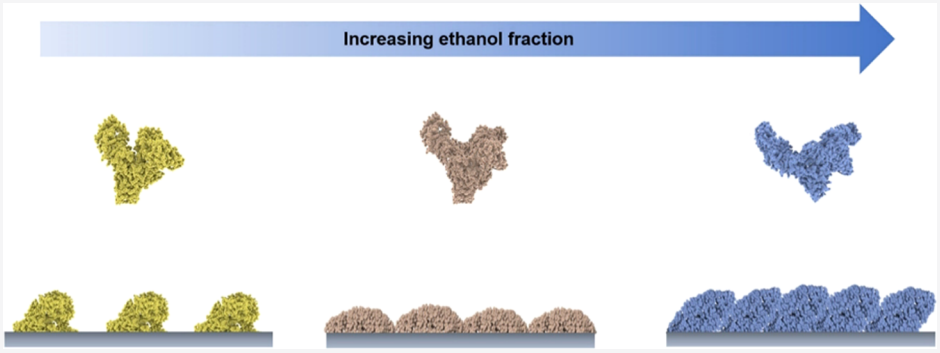

ABSTRACT: Protein adsorption at solid−liquid interfaces is highly relevant to a wide range of applications such as biosensors, drug delivery, and pharmaceuticals. Understanding how protein conformation in bulk solution impacts adsorption behavior is fundamentally important and could also lead to the development of improved protein-based coatings. To date, relevant studies have been conducted in aqueous solutions, while it remains largely unknown how organic solvents and more specifically solvent-induced conformational changes might influence protein adsorption. Herein, using the quartz crystal microbalance-dissipation (QCM-D) and localized surface plasmon resonance (LSPR) techniques, we systematically investigated the real-time adsorption behavior of bovine serum albumin (BSA) protein onto silica surfaces in different water−ethanol mixtures ranging from 0 to 60% (v/v) ethanol. The results showed that there was greater protein adsorption at higher ethanol fractions in the 10−30% range, while more complex adsorption profiles were observed in the 40−60% range. The combination of QCM-D and LSPR measurements led us to further identify specific cases in water−ethanol mixtures where washing steps caused densification of the adsorbed protein layer as opposed to typical desorption of weakly adsorbed molecules in aqueous conditions. We discuss mechanistic factors that drive these overall adsorption trends by taking into account how ethanol fraction affects BSA conformation in bulk solution. Together, our findings demonstrate that BSA proteins can adsorb onto silica surfaces across a wide range of water−ethanol mixture conditions, while specific adsorption profiles depended on the ethanol fraction in a manner closely linked to solution-phase conformational properties.

INTRODUCTION

The formation of protein coatings at solid−liquid interfaces is broadly relevant to numerous applications such as biosensors,[1,2] drug delivery,[3] and biofuel production.[4] A well-defined protein adlayer is often desirable as an interfacial component to increase the functional capability of a material surface in line with the nanoarchitectonic concept (e.g., antifouling coating[5,6] or enzymatic catalysis[7]). Depending on the application, various immobilization strategies have been devised based on noncovalent and covalent chemistries and it is desirable to control the structure and function of protein molecules within the coating layer. However, modulating the conformational properties of adsorbed protein molecules is challenging because proteins typically have weakly folded structures, which are dictated by intramolecular forces, and relatively modest perturbations such as protein−solvent and protein−surface interactions can dramatically influence the protein structure.[8,9]

In general, the noncovalent adsorption of individual protein molecules proceeds via the following mechanistic steps: (1) bulk diffusion toward the interface;[10] (2) surface adsorption; and (3) adsorption-related conformational changes, including unfolding and denaturation, which are linked to protein spreading.[11−13] Accordingly, experimental studies have revealed how a wide range of parameters such as the protein

Received: May 18, 2020
Revised: July 3, 2020
Published: July 11, 2020

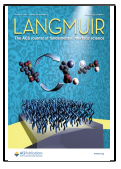

https://dx.doi.org/10.1021/acs.langmuir.0c01478
Langmuir 2020, 36, 9215−9224

structure (e.g., size, shape, conformation) and environmental conditions (e.g., temperature, pH, ionic strength, substrate) affect protein adsorption.[11,14−16] Within this scope, there is growing attention to how the solution-phase conformational stability of a protein—often interpreted relatively in terms of chemical or thermal denaturation profiles or the degree of secondary structure elements in fundamental and applied contexts[17]—affects the extent of protein unfolding in the adsorbed state.

Using a protein engineering approach, Karlsson et al. first demonstrated that human carbonic anhydrase II protein variants with greater conformational stability undergo less denaturation in the adsorbed state and, thus, adsorb more weakly to solid surfaces.[18] This concept has also been applied to bovine serum albumin (BSA), which is one of the most widely studied proteins for surface passivation applications and a member of the serum albumin family that is utilized for various human therapeutic applications. It has been experimentally demonstrated that, at higher temperatures (up to ∼55 °C), BSA exhibits lower solution-phase conformational stability due to unfolding of its α-helical structure and, thus, denatures more in the adsorbed state.[19] In addition, Ma et al. reported that fatty acid-free BSA proteins exhibit better surface passivation properties than fatty acid-containing BSA proteins on account of differences in solution-phase conformational stability and protein spreading on the surface.[20]

To date, all protein adsorption studies related to the topic of solution-phase conformational stability have been conducted in fully aqueous conditions, while there is growing attention to the structure and function of proteins in nonaqueous conditions in general, including in areas such as enzymology, pharmaceuticals, and protein purification.[21,22] For example, ethanol is a protein precipitant that is widely used in plasma fractionation protocols to yield therapeutic proteins from blood[23,24] and can also be used as a solvent to lower the viscosity of antibody formulations.[25] These important applications have spurred interest in understanding how ethanol and other organic solvents affect protein adsorption at solid−liquid interfaces.

In the context of capillary electrophoresis method development, Staub et al. reported that incorporating 5−60% (v/v) fractions of three different, water-miscible organic solvents—acetonitrile, ethanol, and methanol—into the running buffer tended to inhibit protein adsorption onto fused-silica capillaries, although performance outcomes varied depending on the protein and required case-by-case evaluation.[26] In more fundamental studies, Song and Forciniti observed that the addition of 5% (v/v) methanol inhibited the adsorption of human serum albumin onto polystyrene surfaces but did not affect immunoglobulin G adsorption.[27] Achaerandio et al. further investigated the effects of 0−12% (v/v) ethanol on protein adsorption onto bentonite surfaces.[28] It was noted that, with the increasing ethanol fraction, BSA and lysozyme tended to have higher adsorption capacities, while there was no effect on ovalbumin adsorption. At liquid−air interfaces, Puff et al. have also reported greater β-casein protein adsorption with the increasing ethanol fraction in the range of 0−20% (v/v).[29] On the other hand, Rodríguez Niño et al. reported that higher ethanol fractions in the range of 0−12% (v/v) tended to reduce BSA adsorption at liquid−air interfaces.[30] Collectively, these previous studies demonstrate the breadth of how organic solvents can either enhance, inhibit, or have a negligible effect on protein adsorption while highlighting the outstanding need to rationalize how organic solvents affect solution-phase conformational stability and in turn influence protein adsorption at solid−liquid interfaces.

Herein, we systematically investigated BSA protein adsorption onto silica surfaces in different water−ethanol mixtures ranging from 0 to 60% (v/v) ethanol and obtained key insights into how the ethanol fraction affects protein adsorption in water−ethanol mixtures and resulting thin film adsorbate properties in aqueous buffer solution. The quartz crystal microbalance-dissipation (QCM-D) and localized surface plasmon resonance (LSPR) sensing techniques were used as label-free measurement tools to track real-time protein adsorption kinetics and uptake. The QCM-D technique is sensitive to the mass and viscoelastic properties of adsorbed protein molecules and hydrodynamically coupled solvent,[31,32] while the LSPR technique is sensitive to the mass and conformational properties of adsorbed protein molecules only.[33] In addition, we interpreted our experimental results by analyzing circular dichroism spectroscopy data from the literature[34] and discovered that the solution-phase conformational stability of BSA proteins in water−ethanol mixtures plays a critical role in modulating adsorption behavior.

MATERIALS AND METHODS

Protein Sample Preparation. BSA protein (catalog no. A7030) was obtained from Sigma-Aldrich (St. Louis, MO). The lyophilized protein was dissolved in water−ethanol mixtures (between 0 and 60% (v/v) ethanol, in 10% increments) and the protein concentration was fixed at 6.6 mg/mL (100 μM) for all protein solutions. The water−ethanol mixtures were prepared using deionized water and the solution pH of water−ethanol mixtures in the range of 0−60% ethanol fractions has been reported to be in the range of 7−7.4.[35,36] The deionized water was prepared using a Milli-Q water purification system (MilliporeSigma, Burlington, MA). The protein samples were filtered through a polyethersulfone membrane filter with 0.2 μm diameter pores (Thermo Fisher Scientific, catalog no. 595−4520) and stored at 4 °C until use.

Quartz Crystal Microbalance-Dissipation (QCM-D). QCM-D experiments were conducted using a Q-Sense E4 instrument (Biolin Scientific AB, Stockholm, Sweden). The QCM-D sensor chips had a thin, sputter-coated silica coating and a fundamental resonance frequency of 5 MHz (QSX303, Biolin Scientific AB). QCM-D resonance frequency (Δf) and energy dissipation (ΔD) shifts at several odd overtones were recorded as a function of time with a time resolution of 0.9 Hz, and data collection was completed using the Q-Soft software program (Biolin Scientific AB). Data processing was completed using the Q-Tools (Biolin Scientific AB) and OriginPro (OriginLab, Northampton, MA) software programs, and normalized data at the fifth overtone are reported. A peristaltic pump (Reglo Digital MS-4/6, Ismatec, Glattsburg, Switzerland) was used to inject liquid samples into the measurement chamber at a volumetric flow rate of 100 μL/min. Before experiment, the sensor surface was prepared by sequential rinsing with 1% (w/v) aqueous sodium dodecyl sulfate (SDS) solution, deionized water, and ethanol, followed by nitrogen gas drying. To remove any residual organic contaminants and render the silica surface hydrophilic, the sensor chip was then treated with oxygen plasma for 1 min at 50 W radiofrequency power using a CUTE-1MPR machine (Femto Science Inc., Hwaseong, Republic of Korea). All experiments were conducted at 25 °C.

Localized Surface Plasmon Resonance (LSPR) Sensing. LSPR experiments were conducted using an Insplorion XNano instrument (Insplorion AB, Gothenburg, Sweden). The LSPR sensor chips consisted of a gold nanodisk array on a transparent glass substrate and sputter-coated with a 10 nm thick silicon nitride film with a silica overlayer. The nanodisks had a low surface coverage and random, noninteracting arrangement, and the nanodisk dimensions

https://dx.doi.org/10.1021/acs.langmuir.0c01478
Langmuir 2020, 36, 9215−9224

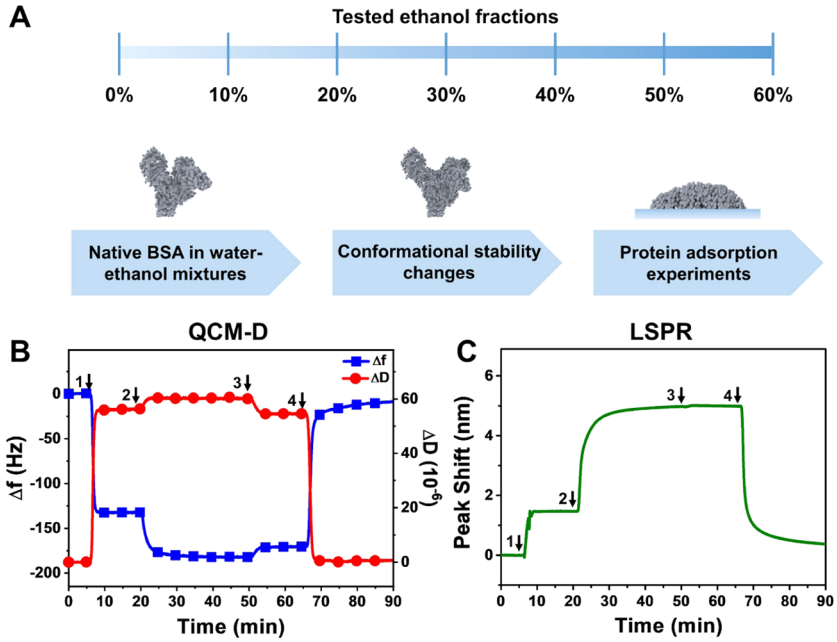

Figure 1. Overview of the measurement approach. (A) Experimental strategy to characterize the effects of BSA protein adsorption in water–ethanol mixtures as a function of ethanol fraction. (B, C) Representative graphs for (B) QCM-D and (C) LSPR experimental protocols using the water–ethanol mixture with 30% (v/v) ethanol. In panel (B), the Δf and ΔD signals are distinguished by square and circle symbol markers, respectively, at selected data points. The baseline signals were initially recorded in the aqueous buffer solution (10 mM Tris, 150 mM NaCl, pH 7.5) before the following steps: (1) exchange to the appropriate water–ethanol mixture; (2) exchange to the equivalent water–ethanol mixture containing 100 μM BSA; (3) wash with the equivalent water–ethanol mixture (without protein); and (4) wash with the aqueous buffer solution.

had a characteristic height and diameter of 20 and 120 nm, respectively. Before experiment, the sensor surface was prepared by sequential rinsing with 1% (w/v) aqueous SDS solution, deionized water, and ethanol, followed by nitrogen gas drying. Then, the sensor chip was treated with oxygen plasma for 1 min at 50 W radiofrequency power using a CUTE-1MPR machine (Femto Science Inc.), which resulted in a hydrophilic silica coating for experiments. After cleaning, the sensor chip was immediately enclosed within a microfluidic chamber and the measurements were performed in an optical transmission mode. Shifts in the maximum-intensity LSPR extinction wavelength ($\Delta\lambda$) were measured as a function of time with a time resolution of 1 Hz. A peristaltic pump (Reglo Digital MS-4/6, Ismatec) was used to inject liquid samples into the measurement chamber at a volumetric flow rate of 100 μL/min. Data collection and processing were completed using the Insplorer (Insplorion AB) and OriginPro software programs, respectively. All experiments were conducted at 25 °C.

RESULTS

Experimental Strategy. Our experimental strategy was motivated by the pioneering work of Griebenow and Klibanov that demonstrated how solution-phase proteins denature in water–organic solvent mixtures compared to those in aqueous solutions and in pure organic solvents.[37] Controlling the extent of protein denaturation depending on the solvent conditions thus provides a useful approach to study the adsorption of a model protein with varying degrees of conformational stability. We selected BSA in water–ethanol mixtures as a suitable model because the protein is well-studied in terms of solution-phase conformational stability in aqueous conditions, the adsorption behavior of serum albumins in organic solvents, including ethanol, is pertinent to numerous applications, and there is existing data about how the BSA secondary structure changes in water–ethanol mixtures as a function of ethanol fraction. In particular, Yoshikawa et al. reported that BSA denaturation in water–ethanol mixtures exhibited a bimodal character, whereby the α-helical character of BSA was largely stable in 0–20% (v/v) ethanol, decreased progressively in 30–50% (v/v) ethanol, and then increased progressively at 60% (v/v) and higher ethanol fractions.[34]

Guided by this framework, we systematically investigated 100 μM BSA protein adsorption onto hydrophilic silica surfaces in water–ethanol mixtures containing 0–60% (v/v) ethanol fractions in 10% (v/v) increments (Figure 1A). The tested BSA protein concentration is comparable to typical concentrations used in protein adsorption and surface passivation studies,[38−40] while the range of water–ethanol mixtures was selected to encompass the bimodal effects of ethanol on the BSA structure and, thus, cover a wide range of conformational stabilities while ensuring high protein solubility (~151 μM at 60% ethanol; see ref 34). QCM-D measurements were conducted using silica-coated sensor chips to track protein adsorption, and shifts in the resonance frequency (Δf) and energy dissipation (ΔD) were recorded as a function of time, which are related to the hydrodynamically coupled mass and viscoelastic properties of the adlayer, respectively.[41] A representative example of the QCM-D operating protocol is presented in Figure 1B and involved the following steps. An initial baseline in an aqueous buffer solution (10 mM Tris, 150 mM NaCl, pH 7.5) was established, before exchanging the bulk solution with the appropriate water–ethanol mixture (step 1). Then, 100 μM BSA protein in the same water–ethanol mixture was added (step 2), followed by a washing step in the equivalent water–ethanol mixture without protein (step 3). Finally, a washing step with the same aqueous buffer solution was performed (step 4). Note that the Δf and ΔD shifts due to step 1 are caused by changes in the viscosity and density of the bulk solution, and not protein adsorption itself. It is thus important to compare Δf and ΔD shifts only when

https://dx.doi.org/10.1021/acs.langmuir.0c01478
Langmuir 2020, 36, 9215−9224

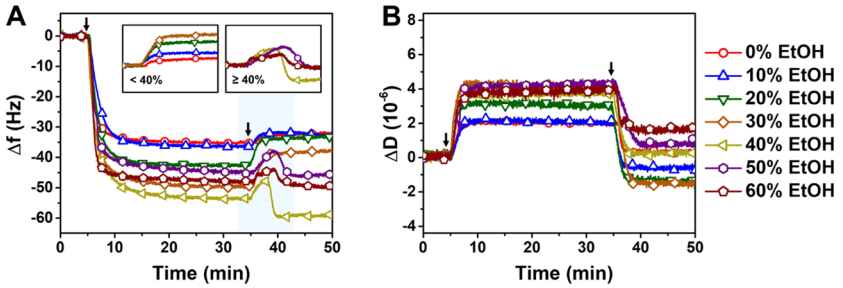

Figure 2. QCM-D measurement of BSA protein adsorption onto silica surfaces in water−ethanol mixtures. Changes in (A) frequency (Δf) and (B) energy dissipation (ΔD) signals are reported as a function of time. The baseline was recorded in the appropriate water−ethanol mixture, and then 100 μM BSA in the equivalent solvent mixture was added under continuous flow conditions from t = 5 min onwards. A washing step in the same solvent mixture (without protein) was performed at around t = 35 min. The solvent cases with different ethanol fractions are represented by 0% (red circles), 10% (blue up-triangles), 20% (green down-triangles), 30% (brown diamonds), 40% (yellow side-triangles), 50% (purple hexagons), and 60% (maroon pentagons). In panel (A), the insets present normalized data for the washing step and the baselines correspond to the adsorbed protein layers before washing.

the initial and final values were recorded in the same bulk solution.[42,43] For this reason, the results of protein adsorption in the water−ethanol mixtures (relative to the water−ethanol baseline without protein, before and after water−ethanol mixture washing) were evaluated along with the final adsorbate properties after aqueous buffer washing (relative to the initial baseline values in aqueous buffer).

We also conducted LSPR experiments to track protein adsorption onto silica-coated gold nanodisk arrays, and shifts in the maximum-intensity extinction wavelength ($\Delta\lambda$) were measured as a function of time, which reflect changes in the local refractive index due to adsorbed BSA molecules on the sensor surface.[33,44] The LSPR operating protocol mirrored the QCM-D protocol, and a representative example is presented in Figure 1C. In general, a larger $\Delta\lambda$ shift typically indicates greater protein adsorption. Note that the $\Delta\lambda$ shifts due to step 1 are caused by changes in the refractive index of the bulk solution, and not protein adsorption itself. The magnitude of the $\Delta\lambda$ shift due to step 1 depends on the bulk refractive index sensitivity of the sensor[45,46] [∼110 nm per refractive index unit (RIU) in our case] and the difference in RIU (ΔRIU) between the refractive indices of the aqueous buffer solution and the water−ethanol mixture. In the representative example, the measurement involves a water−ethanol mixture with 30% (v/v) ethanol and there was a measured $\Delta\lambda$ shift of 1.47 nm due to step 1. The RIU values of the aqueous buffer and 30% ethanol mixture were measured using an Abbe refractometer and determined to be 1.336 and 1.349, respectively, which correspond to a ΔRIU shift of 0.013 and a predicted $\Delta\lambda$ shift of 1.43 nm. Thus, the experimentally observed $\Delta\lambda$ shift agrees well with predictions and verifies LSPR sensor performance.

Control QCM-D and LSPR experiments without BSA protein were also performed to verify that the measurement signals recorded in equivalent bulk solutions, before and after solvent-exchange, were stable in the absence of adsorbed protein. In these control experiments, an aqueous buffer baseline was established, the bulk solution was exchanged to a water−ethanol mixture with 30% ethanol for 1 h, and then the bulk solution was exchanged back to the aqueous buffer solution. Compared to the baseline values, nearly negligible QCM-D Δf and ΔD shifts of less than 2 Hz and $\sim 0 \times 10^{-6}$, respectively, along with an LSPR $\Delta\lambda$ shift of less than 0.05 nm were recorded. These results indicate that there are only very small sensor drifts even after long time spans and repeated solvent-exchanges, confirming that the QCM-D and LSPR measurement signals are stable and reported shifts originate from BSA protein adsorption.

QCM-D Measurements. We initially conducted QCM-D measurements to characterize BSA protein adsorption onto silica surfaces in different water−ethanol mixtures as a function of ethanol (EtOH) fraction. In Figure 2, the normalized Δf and ΔD shifts are presented for the protein adsorption step, whereby the baseline signal was recorded in the appropriate water−ethanol mixture and then 100 μM BSA in the equivalent water−ethanol mixture was added (see the first arrow), followed by washing with the equivalent water−ethanol mixture (without protein; see the second arrow).

In pure water (0% ethanol), BSA adsorption yielded Δf and ΔD shifts of -35.2 ± 0.14 and $1.90 \pm 0.14 \times 10^{-6}$ Hz, respectively, and was mainly irreversible (Figure 2, red circles). Similar adsorption behavior was observed in 10% ethanol, with Δf and ΔD shifts of -36.3 ± 0.35 and $1.85 \pm 0.07 \times 10^{-6}$ Hz, respectively (Figure 2, blue up-triangles). On the other hand, there was greater protein adsorption in the range of 20−30% ethanol. In 20% ethanol, the Δf and ΔD shifts corresponding to protein adsorption were -42.9 ± 0.14 and $2.90 \pm 0.00 \times 10^{-6}$ Hz, respectively (Figure 2, green down-triangles). Greater levels of protein adsorption were observed in 30% ethanol, with Δf and ΔD shifts of -50.4 ± 0.63 and $3.95 \pm 0.21 \times 10^{-6}$ Hz, respectively (Figure 2, brown diamonds). Notably, there was a greater degree of protein desorption upon the solvent washing step (see left inset of Figure 2A).

By contrast, a distinct pattern of adsorption behavior was observed in ≥40% ethanol. In 40% ethanol, the amount of protein adsorption was similar to the 30% ethanol case, with Δf and ΔD shifts of -52.8 ± 0.85 and $3.60 \pm 0.00 \times 10^{-6}$ Hz, respectively (Figure 2, yellow side-triangles). However, the solvent washing step yielded a more complex response, whereby the Δf signal transiently increased before further decreasing and resulted in a larger Δf shift magnitude, which likely reflects a structural reorganization of adsorbed protein molecules on the silica surface (see the right inset of Figure 2A). In 50% ethanol, there was less extensive protein adsorption and the corresponding Δf and ΔD shifts were -45.3 ± 0.42 and $3.75 \pm 0.78 \times 10^{-6}$ Hz, respectively (Figure 2, purple hexagons). Similar measurement responses were observed for protein adsorption in 60% ethanol, and the corresponding Δf and ΔD shifts were -47.6 ± 0.42 and $3.70 \pm 0.14 \times 10^{-6}$ Hz, respectively (Figure 2, maroon pentagons). Thus, the most extensive protein adsorption occurred in 40%

https://dx.doi.org/10.1021/acs.langmuir.0c01478
Langmuir 2020, 36, 9215−9224

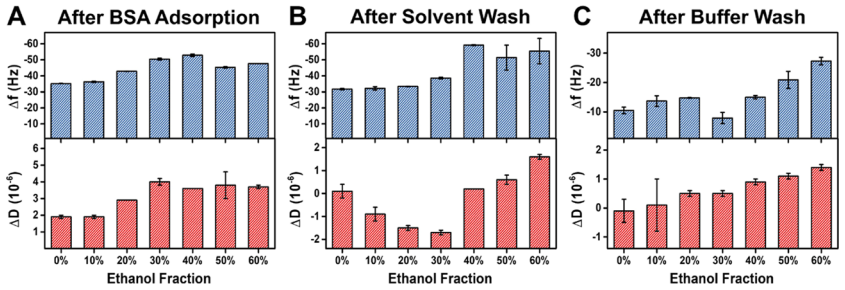

Figure 3. Summary of QCM-D measurement results for protein adsorption in water−ethanol mixtures. Final Δf and ΔD shifts as a function of ethanol fraction in the water−ethanol mixture for (A) BSA adsorption in water−ethanol mixtures (relative to the baseline in the organic-water mixture), (B) BSA adsorption in water−ethanol mixtures after washing with equivalent solvent mixtures (relative to the baseline in the organic-water mixture), and (C) the final BSA adlayer after the second washing step with the aqueous buffer solution (relative to the initial baseline in the aqueous buffer solution). Data are reported as mean ± standard deviation from at least two repeated measurements.

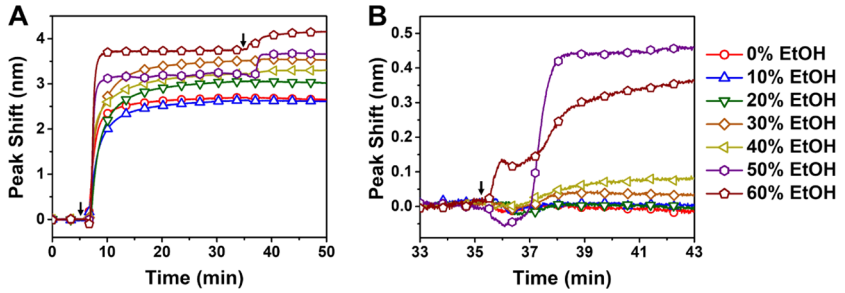

Figure 4. LSPR measurement of BSA protein adsorption onto silica-coated gold nanodisk arrays in water−ethanol mixtures. (A) Changes in the $\Delta\lambda$ signal are reported as a function of time. The baseline was recorded in the appropriate water−ethanol mixture, and then 100 μM BSA in the equivalent solvent mixture was added under continuous flow conditions from t = 5 min onwards. A washing step in the same solvent mixture (without protein) was performed at around t = 35 min. (B) Magnified view of normalized $\Delta\lambda$ data for the water−ethanol mixture washing step and the baselines correspond to the adsorbed protein layers before washing. Data is from panel (A). The solvent cases with different ethanol fractions are represented by 0% (red circles), 10% (blue up-triangles), 20% (green down-triangles), 30% (brown diamonds), 40% (yellow side-triangles), 50% (purple hexagons), and 60% (maroon pentagons).

ethanol and there were two distinct regimes of adsorption behavior: solvents with lower ethanol fractions (10−30%) and solvents with higher ethanol fractions (40−60%).

The QCM-D measurement trends for protein adsorption in the water−ethanol mixtures are summarized in Figure 3. Figure 3A presents the Δf and ΔD shift values corresponding to protein adsorption in the water−ethanol mixtures, relative to the baseline signal in the equivalent water−ethanol solvent mixture alone. Protein adsorption in 0−10% ethanol yielded similar Δf and ΔD shifts. By contrast, larger Δf shifts occurred for protein adsorption in solvents with the increasing ethanol content from 20 to 40%. A similar trend was observed for the ΔD shifts in the 20 and 30% ethanol conditions, while the ΔD shift magnitude plateaued at around 30−40% ethanol. Modestly smaller Δf shifts occurred due to protein adsorption in 50 and 60% ethanol, while the ΔD shifts were similar to the 30−40% ethanol cases.

Figure 3B presents the Δf and ΔD shifts corresponding to the final values for protein adsorption in the water−ethanol mixtures after a washing step in the equivalent solvent mixture was performed, relative to the baseline signal in the equivalent water−ethanol solvent mixture alone. Thus, the reported values correspond to the irreversibly adsorbed protein molecules only. In this case, the final Δf shifts for protein adsorption in 0−30% ethanol were largely similar, while the final ΔD shifts decreased at higher ethanol fractions within this range. In some cases, negative ΔD shifts were observed relative to the baseline signal in the water−ethanol solvent mixture, which is likely related to preferential water attraction by the BSA adlayer. Indeed, such effects would cause the interfacial viscosity of the BSA adlayer to be lower than the viscosity of the bulk solution, which would give rise to a negative ΔD shift.[47] On the other hand, the final Δf shifts for protein adsorption in 40−60% ethanol were generally larger with similar magnitudes in all cases. Notably, the final ΔD shifts for protein adsorption in 40−60% ethanol were moderately larger and also tended to increase in magnitude at higher ethanol fractions in this range. Due to the relatively low ΔD shifts after solvent washing in all cases, the range of acoustic mass values for the BSA adlayers, inclusive of adsorbed protein molecules and hydrodynamically coupled solvent molecules, was estimated based on the Sauerbrey relationship.[48] The calculated acoustic mass values were around ∼600, ∼1050, and ∼950 ng/cm^2 for BSA adlayers in water−ethanol mixtures with 0−30, 40, and 50−60% ethanol fractions, respectively, indicating greater adsorption uptake at higher ethanol fractions in general.

After the washing step with the appropriate water−ethanol mixture, an additional washing step was performed with the aqueous buffer solution (cf. Figure 1, step 4). Figure 3C presents the final Δf and ΔD shift values after the buffer washing step, relative to the baseline signal in the aqueous buffer solution at the beginning of the QCM-D measurement run (cf. Figure 1, baseline). Modest Δf shifts around −10 to −15 Hz were observed for the final protein adlayers that had been initially formed in the 0−20% ethanol range, which are much smaller shifts than typical values around −35 Hz for BSA adlayers that are directly formed on silica surfaces in aqueous

https://dx.doi.org/10.1021/acs.langmuir.0c01478
Langmuir 2020, 36, 9215−9224

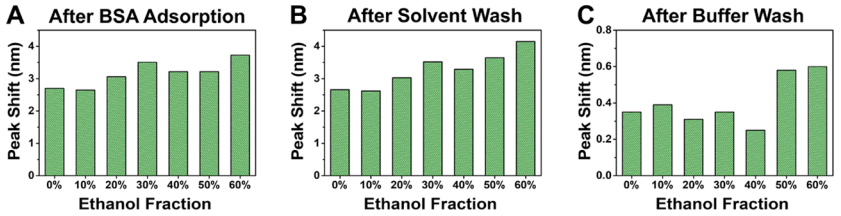

Figure 5. Summary of LSPR measurement results for protein adsorption in water−ethanol mixtures. Final $\Delta\lambda$ shifts as a function of ethanol fraction in the water−ethanol mixture for (A) BSA adsorption in water−ethanol mixtures (relative to the baseline in the organic-water mixture), (B) BSA adsorption in water−ethanol mixtures after washing with equivalent solvent mixtures (relative to the baseline in the organic-water mixture), and (C) the final BSA adlayer after the second washing step with the aqueous buffer solution (relative to the initial baseline in the aqueous buffer solution).

buffer conditions.[16] Notably, the final ΔD shifts corresponding to the protein adlayers formed in 0−20% ethanol were nearly zero, indicating tight coupling of adsorbed protein molecules to the silica surface and these values are much smaller than the typically observed ΔD shifts of 4×10^{-6} for BSA adlayers that are directly formed on silica surfaces in aqueous buffer conditions.[16] Interestingly, very small Δf shifts were also observed for protein adlayers that had been formed in 30% ethanol, with around −5 Hz shifts and small ΔD shifts as well. For protein adlayers formed in 40% and higher ethanol fractions, the final Δf shifts in the aqueous buffer conditions became larger with the increasing ethanol fraction and ranged from around −15 to −28 Hz for the 40−60% ethanol cases, respectively. The corresponding final ΔD shifts were around 1×10^{-6}. Overall, the QCM-D results support that protein deposition in 50−60% ethanol resulted in protein adlayers in the aqueous buffer solution that corresponded to larger Δf and ΔD shifts, as opposed to those initially formed in 0−40% ethanol conditions.

LSPR Measurements. While QCM-D measurements are sensitive to adsorbed protein molecules and hydrodynamically coupled solvent molecules, we also performed LSPR measurements that are sensitive to the adsorption of protein molecules only. Experimentally, BSA protein adsorption onto silica-coated gold nanodisk arrays was tracked in different water−ethanol mixtures as a function of ethanol (EtOH) fraction. Figure 4A presents the LSPR data for protein adsorption, and the normalized $\Delta\lambda$ shifts are shown for the protein adsorption step. The baseline signal was recorded in the appropriate water−ethanol mixture, and then 100 μM BSA in the equivalent water−ethanol mixture was added (see the first arrow), followed by washing with the equivalent water−ethanol mixture (without protein; see the second arrow).

In 0 and 10% ethanol, similar levels of protein adsorption were observed with $\Delta\lambda$ shifts around 2.70 nm and 2.65 nm, respectively (Figure 4A, red circles and blue triangles). At higher ethanol fractions, there was greater protein adsorption and the final $\Delta\lambda$ shifts were 3.06 nm and 3.51 nm in 20 and 30% ethanol, respectively (Figure 4A, green triangles and brown diamonds). On the other hand, in 40 and 50% ethanol, the $\Delta\lambda$ shifts reached around 3.22 nm (Figure 4A, yellow triangles and purple hexagons). The most extensive protein adsorption occurred in 60% ethanol, and the $\Delta\lambda$ shift was 3.73 nm (Figure 4A, maroon pentagons). A magnified view of the solvent washing step data in Figure 4B further revealed ethanol fraction-dependent protein adsorption and stability. Specifically, protein adsorption in 0−20% ethanol was mainly irreversible, while there were slight increases of <0.1 nm in the $\Delta\lambda$ shift for adsorbed protein layers in 30−40% ethanol, which indicated that the adsorbed protein molecules, on average, become closer to the sensor surface.[19] More pronounced changes due to solvent washing occurred in 50 and 60% ethanol, in which cases there were additional $\Delta\lambda$ shifts of >0.3 nm. While solvent washing steps typically cause protein desorption in aqueous buffer solutions, these results support that solvent washing in water−ethanol mixtures can cause densification of adsorbed protein layers.

The LSPR measurement trends for protein adsorption in the water−ethanol mixtures are summarized in Figure 5. Figure 5A presents the $\Delta\lambda$ shift values corresponding to protein adsorption in the water−ethanol mixtures, relative to the baseline signal in the equivalent water−ethanol solvent mixture alone. Protein adsorption in 0−10% ethanol yielded similar $\Delta\lambda$ shifts, while the $\Delta\lambda$ shifts were larger in 20−30% ethanol. Modestly smaller shifts were observed in 40−50% ethanol, while the larger shifts occurred in 60% ethanol. We also compared the $\Delta\lambda$ shifts after a solvent washing step, which corresponds to the final values for protein adsorption in the water−ethanol mixtures after a washing step in the equivalent solvent mixture was performed, relative to the baseline signal in the equivalent water−ethanol solvent mixture alone (Figure 5B). The overall trend was largely similar to the trend in protein adsorption at saturation (cf. Figure 5A), and it was noteworthy that the magnitudes of the $\Delta\lambda$ shifts were generally larger after the solvent washing step, which indicates a structural reorganization of adsorbed protein molecules on the silica surface.

Using the Lorentz−Lorenz equation,[49−51] the measurement responses were converted into optical mass values (adsorbed protein molecules only), which were determined to be around ∼480, ∼590, and ∼720 ng/cm^2 for BSA adlayers in water−ethanol mixtures with 0−30, 40, and 50−60% ethanol fractions, respectively (see calculation details in the Supporting Information). The solvent fraction of the BSA adlayers was also determined based on the calculated acoustic and optical mass values, the difference of which reflects the solvent mass. Based on this approach, it was estimated that the solvent fraction was around ∼20, ∼44, and ∼24% for BSA adlayers in water−ethanol mixtures with 0−30, 40, and 50−60% ethanol fractions, respectively. This trend supports that there is a transition in the adsorption behavior for the 40% ethanol case, which is consistent with the marked differences in the QCM-D and LSPR measurement responses starting at this condition as well. The surface coverage of the adsorbed BSA proteins in the different water−ethanol mixtures was also determined based on the LSPR measurement responses and tended to increase from around 49 to 93% for BSA adlayers in water−ethanol mixtures with 0−60% ethanol fractions (see the Supporting

https://dx.doi.org/10.1021/acs.langmuir.0c01478
Langmuir 2020, 36, 9215−9224

Information and Table S1). This trend indicates that the BSA adlayer packing density increases at higher ethanol fractions in general.

After the solvent washing step, an additional washing step was performed with the aqueous buffer solution (cf. Figure 1, step 4). Figure 5C presents the final $\Delta\lambda$ shift values after the buffer washing step, relative to the baseline signal in the aqueous buffer solution at the beginning of the LSPR measurement run (cf. Figure 1, baseline). In general, the final $\Delta\lambda$ shift values were around <0.4 and >0.5 nm for protein adlayers that had been initially formed in the 0−40 and 50−60% ethanol ranges, respectively. These data agree well with the QCM-D data and support that the ethanol-induced conformational changes can have significant effects on protein adsorption and related structural transformations in water−ethanol mixtures, while the resulting adlayers demonstrate low stability when the bulk solution is exchanged to the aqueous buffer solution.

DISCUSSION

To analyze the QCM-D and LSPR results, it is important to take into account how the solution-phase BSA conformational structure changes as a function of the ethanol fraction in the water−ethanol mixtures. For solution-phase BSA in water−ethanol mixtures, Yoshikawa et al. have presented CD spectroscopy data[34] that provides insight into how the BSA secondary structure depends on the ethanol fraction and we interpret our QCM-D and LSPR adsorption data within this context. More specifically, for 0−20% (v/v) ethanol, Yoshikawa et al. observed that the solution-phase BSA structure largely retains the native conformation that is found in aqueous conditions. As the ethanol fraction rises from 30 to 50% (v/v), there is a marked decrease in α-helicity, in turn decreasing BSA conformational stability due to protein unfolding. On the other hand, at 60% (v/v) ethanol, there is partial, but still relatively low, induction of α-helical character in solution-phase BSA proteins along with the possible formation of β-sheet secondary structures.[34] Thus, BSA conformational structure in water−ethanol mixtures exhibits a bimodal character, likely due to the following two competing factors: (1) higher ethanol fraction conditions increase the tendency of protein molecules to denature[52,53] and (2) lower water fraction reduces protein conformational flexibility, in turn restricting the protein from structurally transforming into the lowest energy conformation.[37,54]

Figure 6 presents a schematic illustration of this trend along with the corresponding adsorption behavior. In the schematic illustration and in our analysis, the BSA protein adlayer is treated as a monolayer because (1) the adsorption of BSA monomers typically leads to monolayer formation in past studies,[16,55] (2) there are relatively small QCM-D ΔD shifts upon solvent washing, while the corresponding shifts for multilayers are usually much larger;[56,57] and (3) there is a gradual increase in the adsorption uptake at higher ethanol fractions rather than a sharp increase, which typically indicates a transition from monolayer to multilayer adsorption.[19,58] Below, we discuss trends in the experimental data from the complementary QCM-D and LSPR techniques while also taking into account ethanol-induced changes in protein secondary structure across different ethanol fractions. We note that the QCM-D measurements are sensitive to the adsorbed protein molecules and hydrodynamically coupled

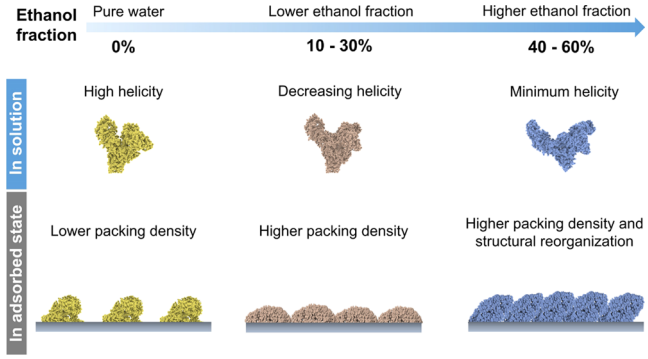

Figure 6. Schematic illustration of solution-phase BSA proteins in water−ethanol mixtures as a function of ethanol fraction and corresponding adsorption behavior trends. In pure water, BSA exhibits a mainly α-helical, native conformation in the solution phase and adsorbed BSA molecules form an adlayer (monolayer) with relatively low packing density. With the increasing ethanol fraction (10−30%), there is a tendency for BSA proteins to have decreased helicity and lower conformational stability, which results in adsorbed BSA layers that have higher packing density. At higher ethanol fractions (40−60%), solution-phase BSA proteins exhibit even lower helicity with a reported minimum helicity at a 50% ethanol fraction and accordingly the adsorbed BSA layers have high packing density and undergo structural reorganization.

solvent molecules, while the LSPR measurements are sensitive to the adsorbed protein molecules only.

As expected, similar conformational structures of BSA proteins in 0 and 10% ethanol resulted in similar adsorption behavior and adlayer properties. As the ethanol fraction increased from 10 to 30%, the QCM-D and LSPR data showed increased adsorption uptake, both at saturation and after a solvent washing step. In line with the solution-phase conformational data, these findings indicate that BSA molecules exhibited more conformational flexibility on account of partial unfolding, resulting in more well-packed adlayers upon adsorption.[13,59] In this regime, the tendency of protein molecules to denature with the increasing ethanol fraction appeared to be the dominant factor. In particular, ethanol solvates hydrophobic side chains in BSA[60] and weakens long-range intramolecular interactions between α-helices,[61] which causes a reduction in the α-helical character. The resulting increased conformational flexibility typically leads to greater protein deformation and spreading in the adsorbed state. Often, such behavior is accompanied by less total uptake due to differences in the adsorption footprint of individual protein molecules;[62] however, interestingly, we observed a moderate tendency for the total uptake and hence surface coverage to increase as well. This observation suggests that the formation of well-packed BSA adlayers is aided by strong interactions between adsorbed proteins, possibly due to greater ethanol-induced exposure of side chains.

On the other hand, a distinct trend in adsorption behavior was observed at 40% and higher ethanol fractions. Interestingly, the QCM-D Δf shift due to protein adsorption increased from 30 to 40% ethanol fraction, while the corresponding LSPR $\Delta\lambda$ shift decreased, implying that the adsorbed BSA layer had a different structural configuration in this condition. This scenario is supported by the complex response profile observed in the time-resolved Δf shift, and a higher final ΔD shift upon solvent washing further indicates structural reorganization of the adsorbed BSA molecules. At 40%

https://dx.doi.org/10.1021/acs.langmuir.0c01478
Langmuir 2020, 36, 9215−9224

ethanol, both ethanol-induced protein denaturation and lower conformational flexibility of BSA molecules in the relatively water-poor environment appear to drive complex adsorption behavior. Specifically, the larger Δf shift observed in this condition suggests that BSA protein molecules adopted a more elongated structure due to extensive ethanol-induced denaturation, leading to adsorption along the shorter axis that would result in a smaller footprint and, therefore, a higher total uptake. Adsorption-related protein denaturation and correspondingly greater exposure of amino acid side chains might also increase the amount of hydrodynamically coupled solvent, in line with the estimated high solvent fraction at this transition condition. At the same time, this packing arrangement caused the BSA molecules to be, on average, further away from the sensor surface, resulting in a decreased $\Delta\lambda$ shift compared to the 30% ethanol case. The reduced adsorption footprint of the adsorbed BSA proteins also contributed to weaker protein−surface interactions, which resulted in more proteins desorbing from the surface upon aqueous buffer washing.

At 50 and 60% ethanol fractions, more extensive structural reorganization of adsorbed BSA layers occurred, as indicated by complex Δf shifts and increased $\Delta\lambda$ shifts upon solvent washing. In this regime, the loss of long-range intramolecular interactions coupled with the increasingly nonpolar solvent environment tended to partially recover α-helicity and reduce flexibility in the solution-phase BSA conformational structure.[34] The tendency toward decreased Δf shifts at 50 and 60% ethanol fractions is consistent with the solution-phase BSA protein molecules reverting back to a predominantly globular shape instead of an elongated structure, and accordingly more globular BSA has an increased adsorption footprint and, thus, decreased total adsorption uptake. This finding is further supported by the increased initial rate of change in the LSPR $\Delta\lambda$ signals at 50 and 60% ethanol fractions, which is possibly due to oligomerization[63] and a greater fraction of irreversibly bound BSA adsorbates.[15,64,65] The larger $\Delta\lambda$ shifts at 50 to 60% ethanol fractions similarly support that the BSA molecule became, on average, closer to the sensor surface with the return to a globular shape, as opposed to the more elongated shape at 40% ethanol fraction. Interestingly, upon solvent washing, the $\Delta\lambda$ signal showed large positive shifts, which points to significant structural rearrangements that likely involve the collapse of adsorbed BSA molecules so that they are, on average, closer to the sensor surface. It is also possible that, prior to solvent washing, some BSA proteins were weakly adsorbed as part of a quasi-multilayer state due to enhanced protein−protein interactions in solvent conditions with higher ethanol fractions. In such cases, weakly adsorbed BSA proteins would desorb upon solvent washing, in part facilitating densification of the BSA adlayer. These interpretations agree with the observed trend that the surface coverage values of BSA adlayers upon solvent washing are greater at higher ethanol fractions, and collectively support that protein adsorption in water−ethanol mixtures with ≥40% ethanol fractions leads to densification of adsorbed BSA protein layers.

CONCLUSIONS

In this study, we conducted QCM-D and LSPR measurements to track BSA adsorption onto silica surfaces as a function of ethanol fraction in different water−ethanol mixtures. Our findings revealed that protein adsorption increased at higher ethanol fractions within the 10−30% range, while more complex adsorption profiles were observed in the 40−60% range, including more extensive structural rearrangements upon washing. While washing, to remove weakly adsorbed protein molecules, typically results in some desorption in aqueous conditions, we observed specific conditions in water−ethanol mixtures where there was instead densification of the adsorbed protein layer upon washing, as indicated by larger measurement responses. To interpret the adsorption data, we considered how ethanol fraction affects protein conformation in bulk solution and discovered that ethanol-induced protein conformational changes were closely related to the trends in adsorption behavior. In particular, at lower ethanol fractions, increased adsorption occurred as the result of greater protein unfolding in solution as well as stronger protein−protein interactions in the adsorbed state. On the other hand, at higher ethanol fractions, more extensive changes in the solution-phase protein conformation influenced the adsorption pathway and impacted the molecular footprint of adsorbed proteins accordingly. Importantly, these two distinct adsorption regimes are closely related to how ethanol fraction influences protein unfolding in water−ethanol mixtures, whereby a critical extent of unfolding occurs around 30−40% ethanol. Taken together, our findings demonstrate how ethanol-induced conformational changes in the BSA protein structure can modulate the extent of protein adsorption onto silica surfaces and more broadly highlight how solution-phase conformational stability is an important factor in dictating how proteins adsorb and denature at solid−liquid interfaces.

ASSOCIATED CONTENT

Supporting Information

The Supporting Information is available free of charge at https://pubs.acs.org/doi/10.1021/acs.langmuir.0c01478.

Calculation of BSA adlayer surface coverage from LSPR measurements; calculation of the optical mass of the BSA adlayer from LSPR measurements; list of values for the solvent RI, LSPR measurement response after solvent washing, effective RI of BSA adlayers, and the surface coverage of adsorbed BSA proteins for water−ethanol mixtures at all tested ethanol fractions (Table S1) (PDF)

AUTHOR INFORMATION

Corresponding Authors

Nam-Joon Cho − *School of Materials Science and Engineering, Nanyang Technological University, 639798, Singapore;* orcid.org/0000-0002-8692-8955; Email: njcho@ntu.edu.sg

Joshua A. Jackman − *School of Chemical Engineering, Sungkyunkwan University, Suwon 16419, Republic of Korea;* orcid.org/0000-0002-1800-8102; Email: jjackman@skku.edu

Authors

Jia Ying Brenda Tan − *School of Chemical Engineering, Sungkyunkwan University, Suwon 16419, Republic of Korea; School of Materials Science and Engineering, Nanyang Technological University, 639798, Singapore*

Bo Kyeong Yoon − *School of Chemical Engineering, Sungkyunkwan University, Suwon 16419, Republic of Korea*

Gamaliel Junren Ma − *School of Materials Science and Engineering, Nanyang Technological University, 639798, Singapore*

https://dx.doi.org/10.1021/acs.langmuir.0c01478
Langmuir 2020, 36, 9215−9224

Tun Naw Sut − *School of Chemical Engineering, Sungkyunkwan University, Suwon 16419, Republic of Korea; School of Materials Science and Engineering, Nanyang Technological University, 639798, Singapore*

Complete contact information is available at: https://pubs.acs.org/10.1021/acs.langmuir.0c01478

Author Contributions

[§]J.Y.B.T. and B.K.Y. contributed equally to this work.

Notes

The authors declare no competing financial interest.

■ ACKNOWLEDGMENTS

This work was supported by the National Research Foundation of Korea (NRF) grant funded by the Korean government (MSIT) (No. 2020R1C1C1004385). In addition, this work was supported by the Korea Research Fellowship Program through the National Research Foundation of Korea (NRF) funded by the Ministry of Science and ICT (2019H1D3A1A01070318). The authors acknowledge the support of OmniColab Ltd. (Suwon, Republic of Korea) for allowing the use of a QCM-D instrument.

■ REFERENCES

(1) Bhakta, S. A.; Evans, E.; Benavidez, T. E.; Garcia, C. D. Protein adsorption onto nanomaterials for the development of biosensors and analytical devices: a review. *Anal. Chim. Acta* **2015**, *872*, 7−25.

(2) Choi, S.; Chae, J. A microfluidic biosensor based on competitive protein adsorption for thyroglobulin detection. *Biosens. Bioelectron.* **2009**, *25*, 118−123.

(3) Schöttler, S.; Becker, G.; Winzen, S.; Steinbach, T.; Mohr, K.; Landfester, K.; Mailänder, V.; Wurm, F. R. Protein adsorption is required for stealth effect of poly (ethylene glycol)-and poly (phosphoester)-coated nanocarriers. *Nat. Nanotechnol.* **2016**, *11*, 372−377.

(4) Ahmad, R.; Sardar, M. Enzyme immobilization: an overview on nanoparticles as immobilization matrix. *Biochem. Anal. Biochem.* **2015**, *4*, 178.

(5) Ariga, K.; Li, J.; Fei, J.; Ji, Q.; Hill, J. P. Nanoarchitectonics for dynamic functional materials from atomic-/molecular-level manipulation to macroscopic action. *Adv. Mater.* **2016**, *28*, 1251−1286.

(6) Tanaka, M.; Kobayashi, S.; Murakami, D.; Aratsu, F.; Kashiwazaki, A.; Hoshiba, T.; Fukushima, K. Design of polymeric biomaterials: the "intermediate water concept". *Bull. Chem. Soc. Jpn.* **2019**, *92*, 2043−2057.

(7) Ariga, K.; Ji, Q.; Mori, T.; Naito, M.; Yamauchi, Y.; Abe, H.; Hill, J. P. Enzyme nanoarchitectonics: organization and device application. *Chem. Soc. Rev.* **2013**, *42*, 6322−6345.

(8) Lahari, C.; Jasti, L. S.; Fadnavis, N. W.; Sontakke, K.; Ingavle, G.; Deokar, S.; Ponrathnam, S. Adsorption induced enzyme denaturation: the role of polymer hydrophobicity in adsorption and denaturation of α-chymotrypsin on allyl glycidyl ether (AGE)-ethylene glycol dimethacrylate (EGDM) copolymers. *Langmuir* **2010**, *26*, 1096−1106.

(9) Faulón Marruecos, D.; Schwartz, D. K.; Kaar, J. L. Impact of surface interactions on protein conformation. *Curr. Opin. Colloid Interface Sci* **2018**, *38*, 45−55.

(10) Stutz, H. Protein attachment onto silica surfaces—a survey of molecular fundamentals, resulting effects and novel preventive strategies in CE. *Electrophoresis* **2009**, *30*, 2032−2061.

(11) Rabe, M.; Verdes, D.; Seeger, S. Understanding protein adsorption phenomena at solid surfaces. *Adv. Colloid Interface Sci.* **2011**, *162*, 87−106.

(12) Vogler, E. A. Protein adsorption in three dimensions. *Biomaterials* **2012**, *33*, 1201−1237.

(13) Yano, Y. F. Kinetics of protein unfolding at interfaces. *J. Phys.: Condens. Matter* **2012**, *24*, No. 503101.

(14) Vallée, A.; Humblot, V.; Al Housseiny, R.; Boujday, S.; Pradier, C.-M. BSA adsorption on aliphatic and aromatic acid SAMs: Investigating the effect of residual surface charge and sublayer nature. *Colloids Surf., B* **2013**, *109*, 136−142.

(15) Park, J.; Sut, T.; Jackman, J.; Ferhan, A.; Yoon, B.; Cho, N. Controlling adsorption and passivation properties of bovine serum albumin on silica surfaces by ionic strength modulation and cross-linking. *Phys. Chem. Chem. Phys.* **2017**, *19*, 8854−8865.

(16) Park, J. H.; Jackman, J. A.; Ferhan, A. R.; Ma, G. J.; Yoon, B. K.; Cho, N.-J. Temperature-induced denaturation of BSA protein molecules for improved surface passivation coatings. *ACS Appl. Mater. Interfaces* **2018**, *10*, 32047−32057.

(17) Yao, H.; Wynendaele, E.; De Spiegeleer, B. Thermal sensitivity as a quality control attribute for biotherapeutics: The L-asparaginase case. *Drug Test. Anal.* **2020**, *12*, 67−77.

(18) Karlsson, M.; Ekeroth, J.; Elwing, H.; Carlsson, U. Reduction of irreversible protein adsorption on solid surfaces by protein engineering for increased stability. *J. Biol. Chem.* **2005**, *280*, 25558−25564.

(19) Jackman, J. A.; Ferhan, A. R.; Yoon, B. K.; Park, J. H.; Zhdanov, V. P.; Cho, N.-J. Indirect nanoplasmonic sensing platform for monitoring temperature-dependent protein adsorption. *Anal. Chem.* **2017**, *89*, 12976−12983.

(20) Ma, G. J.; Ferhan, A. R.; Jackman, J. A.; Cho, N.-J. Conformational flexibility of fatty acid-free bovine serum albumin proteins enables superior antifouling coatings. *Commun. Mater.* **2020**, *1*, 45.

(21) Klibanov, A. M. Improving enzymes by using them in organic solvents. *Nature* **2001**, *409*, 241−246.

(22) Yoshikawa, H.; Hirano, A.; Arakawa, T.; Shiraki, K. Mechanistic insights into protein precipitation by alcohol. *Int. J. Biol. Macromol.* **2012**, *50*, 865−871.

(23) Cohn, E. J.; Strong, L. E.; Hughes, W.; Mulford, D.; Ashworth, J.; Melin, M.; Taylor, H. Preparation and properties of serum and plasma proteins. IV. A system for the separation into fractions of the protein and lipoprotein components of biological tissues and fluids. *J. Am. Chem. Soc.* **1946**, *68*, 459−475.

(24) Schneider, W.; Lefevre, H.; Fiedler, H.; McCarty, L. J. An alternative method of large scale plasma fractionation for the isolation of serum albumin. *Blut* **1975**, *30*, 121−134.

(25) Srinivasan, C.; Weight, A. K.; Bussemer, T.; Klibanov, A. M. Non-aqueous suspensions of antibodies are much less viscous than equally concentrated aqueous solutions. *Pharm. Res.* **2013**, *30*, 1749−1757.

(26) Staub, A.; Comte, S.; Rudaz, S.; Veuthey, J.-L.; Schappler, J. Use of organic solvent to prevent protein adsorption in CE-MS experiments. *Electrophoresis* **2010**, *31*, 3326−3333.

(27) Song, D.; Forciniti, D. Effects of cosolvents and pH on protein adsorption on polystyrene latex: a dynamic light scattering study. *J. Colloid Interface Sci.* **2000**, *221*, 25−37.

(28) Achaerandio, I.; Pachova, V.; Güell, C.; López, F. Protein adsorption by bentonite in a white wine model solution: effect of protein molecular weight and ethanol concentration. *Am. J. Enol. Vitic.* **2001**, *52*, 122−126.

(29) Puff, N.; Cagna, A.; Aguié-Béghin, V.; Douillard, R. Effect of ethanol on the structure and properties of β-casein adsorption layers at the air/buffer interface. *J. Colloid Interface Sci.* **1998**, *208*, 405−414.

(30) Rodríguez Niño, M. R.; Wilde, P. J.; Clark, D. C.; Husband, F. A.; Rodríguez Patino, J. M. Rheokinetic analysis of protein films at the air−aqueous phase interface. 1. bovine serum albumin adsorption on ethanol aqueous solutions. *J. Agric. Food Chem.* **1997**, *45*, 3010−3015.

(31) Chen, Q.; Xu, S.; Liu, Q.; Masliyah, J.; Xu, Z. QCM-D study of nanoparticle interactions. *Adv. Colloid Interface Sci.* **2016**, *233*, 94−114.

(32) Höök, F.; Vörös, J.; Rodahl, M.; Kurrat, R.; Böni, P.; Ramsden, J.; Textor, M.; Spencer, N.; Tengvall, P.; Gold, J. A comparative study of protein adsorption on titanium oxide surfaces using in situ

ellipsometry, optical waveguide lightmode spectroscopy, and quartz crystal microbalance/dissipation. *Colloids Surf., B* **2002**, *24*, 155−170.
(33) Jackman, J. A.; Ferhan, A. R.; Cho, N. J. Nanoplasmonic sensors for biointerfacial science. *Chem. Soc. Rev.* **2017**, *46*, 3615−3660.
(34) Yoshikawa, H.; Hirano, A.; Arakawa, T.; Shiraki, K. Effects of alcohol on the solubility and structure of native and disulfide-modified bovine serum albumin. *Int. J. Biol. Macromol.* **2012**, *50*, 1286−1291.
(35) Kotrba, M.; Schilling, L.-H. Measurement of pH in Ethanol, Distilled Water, and Their Mixtures: On the Assessment of pH in Ethanol-Based Natural History Wet Collections and the Detrimental Aspects of Dilution with Distilled Water. In *Collection Forum*; Society for the Preservation of Natural History Collections, 2017; Vol. *31*, pp 84−101.
(36) Gelsema, W.; De Ligny, C.; Remijnse, A.; Blijleven, H. pH-measurements in alcohol-water mixtures, using aqueous standard buffer solutions for calibration. *Recl. Trav. Chim. Pays-Bas* **1966**, *85*, 647−660.
(37) Griebenow, K.; Klibanov, A. M. On protein denaturation in aqueous−organic mixtures but not in pure organic solvents. *J. Am. Chem. Soc.* **1996**, *118*, 11695−11700.
(38) Jeyachandran, Y.; Mielczarski, E.; Rai, B.; Mielczarski, J. Quantitative and qualitative evaluation of adsorption/desorption of bovine serum albumin on hydrophilic and hydrophobic surfaces. *Langmuir* **2009**, *25*, 11614−11620.
(39) Jeyachandran, Y.; Mielczarski, J.; Mielczarski, E.; Rai, B. Efficiency of blocking of non-specific interaction of different proteins by BSA adsorbed on hydrophobic and hydrophilic surfaces. *J. Colloid Interface Sci.* **2010**, *341*, 136−142.
(40) Mahmood, T.; Yang, P.-C. Western blot: technique, theory, and trouble shooting. *N. Am. J. Med. Sci.* **2012**, *4*, 429−434.
(41) Cho, N.-J.; Frank, C. W.; Kasemo, B.; Höök, F. Quartz crystal microbalance with dissipation monitoring of supported lipid bilayers on various substrates. *Nat. Protoc.* **2010**, *5*, 1096−1106.
(42) Betlem, K.; Cordoyiannis, G.; Losada-Pérez, P. Supported lipid membranes at the Au-buffer interface by solvent exchange: the effect of initial solvent concentration. *Phys. Status Solidi A* **2019**, No. 1900837.
(43) Neupane, S.; Cordoyiannis, G.; Renner, F. U.; Losada-Pérez, P. Real-time monitoring of interactions between solid-supported lipid vesicle layers and short-and medium-chain length alcohols: ethanol and 1-pentanol. *Biomimetics* **2019**, *4*, 8.
(44) Ferhan, A. R.; Jackman, J. A.; Sut, T. N.; Cho, N.-J. Quantitative comparison of protein adsorption and conformational changes on dielectric-coated nanoplasmonic sensing arrays. *Sensors* **2018**, *18*, 1283.
(45) Dahlin, A. B.; Wittenberg, N. J.; Höök, F.; Oh, S.-H. Promises and challenges of nanoplasmonic devices for refractometric biosensing. *Nanophotonics* **2013**, *2*, 83−101.
(46) Oh, S.-H.; Altug, H. Performance metrics and enabling technologies for nanoplasmonic biosensors. *Nat. Commun.* **2018**, *9*, No. 5263.
(47) Gillissen, J. J.; Jackman, J. A.; Sut, T. N.; Cho, N.-J. Disentangling bulk polymers from adsorbed polymers using the quartz crystal microbalance. *Appl. Mater. Today* **2020**, *18*, No. 100460.
(48) Sauerbrey, G. The use of quartz oscillators for weighing thin layers and for microweighing. *Z. Phys.* **1959**, *155*, 206−222.
(49) Jonsson, M. P.; Dahlin, A. B.; Jönsson, P.; Höök, F. Nanoplasmonic biosensing with focus on short-range ordered nanoholes in thin metal films. *Biointerphases* **2008**, *3*, FD30−FD40.
(50) Ferhan, A. R.; Jackman, J. A.; Cho, N.-J. Integration of quartz crystal microbalance-dissipation and reflection-mode localized surface plasmon resonance sensors for biomacromolecular interaction analysis. *Anal. Chem.* **2016**, *88*, 12524−12531.
(51) Ferhan, A. R.; Spackova, B.; Jackman, J. A.; Ma, G. J.; Sut, T. N.; Homola, J.; Cho, N.-J. Nanoplasmonic ruler for measuring separation distance between supported lipid bilayers and oxide surfaces. *Anal. Chem.* **2018**, *90*, 12503−12511.
(52) Brandts, J. F.; Hunt, L. Thermodynamics of protein denaturation. III. Denaturation of ribonuclease in water and in aqueous urea and aqueous ethanol mixtures. *J. Am. Chem. Soc* **1967**, *89*, 4826−4838.
(53) Bull, H. B.; Breese, K. Interaction of alcohols with proteins. *Biopolymers* **1978**, *17*, 2121−2131.
(54) Rupley, J. A.; Careri, G. Protein Hydration and Function. In *Advances in Protein Chemistry*; Academic Press, 1991; Vol. *41*, pp 37−172.
(55) Jachimska, B.; Tokarczyk, K.; Łapczyńska, M.; Puciul-Malinowska, A.; Zapotoczny, S. Structure of bovine serum albumin adsorbed on silica investigated by quartz crystal microbalance. *Colloids Surf., A* **2016**, *489*, 163−172.
(56) Ma, G. J.; Ferhan, A. R.; Sut, T. N.; Jackman, J. A.; Cho, N.-J. Understanding how natural sequence variation in serum albumin proteins affects conformational stability and protein adsorption. *Colloids Surf., B* **2020**, *194*, No. 111194.
(57) Notley, S. M.; Eriksson, M.; Wågberg, L. Visco-elastic and adhesive properties of adsorbed polyelectrolyte multilayers determined in situ with QCM-D and AFM measurements. *J. Colloid Interface Sci.* **2005**, *292*, 29−37.
(58) Bieker, P.; Schönhoff, M. Linear and exponential growth regimes of multilayers of weak polyelectrolytes in dependence on pH. *Macromolecules* **2010**, *43*, 5052−5059.
(59) Ouberai, M. M.; Xu, K.; Welland, M. E. Effect of the interplay between protein and surface on the properties of adsorbed protein layers. *Biomaterials* **2014**, *35*, 6157−6163.
(60) Nozaki, Y.; Tanford, C. The solubility of amino acids and two glycine peptides in aqueous ethanol and dioxane solutions: establishment of a hydrophobicity scale. *J. Biol. Chem.* **1971**, *246*, 2211−2217.
(61) Gromiha, M. M.; Selvaraj, S. Comparison between long-range interactions and contact order in determining the folding rate of two-state proteins: application of long-range order to folding rate prediction. *J. Mol. Biol.* **2001**, *310*, 27−32.
(62) van der Veen, M.; Stuart, M. C.; Norde, W. Spreading of proteins and its effect on adsorption and desorption kinetics. *Colloids Surf., B* **2007**, *54*, 136−142.
(63) Yoshizawa, S.; Arakawa, T.; Shiraki, K. Dependence of ethanol effects on protein charges. *Int. J. Biol. Macromol.* **2014**, *68*, 169−172.
(64) Zhdanov, V. P.; Kasemo, B. Monte Carlo simulation of the kinetics of protein adsorption. *Proteins* **1998**, *30*, 177−182.
(65) Kwok, K.; Yeung, K.; Cheung, N. Adsorption kinetics of bovine serum albumin on fused silica: population heterogeneities revealed by single-molecule fluorescence microscopy. *Langmuir* **2007**, *23*, 1948−1952.

https://dx.doi.org/10.1021/acs.langmuir.0c01478
Langmuir 2020, 36, 9215−9224